

1  
2  
3  
4 **Vortex fluidics-mediated DNA rescue from formalin-fixed museum**  
5 **specimens**  
6

7 Christian A. Totoiu<sup>1, #a</sup>, Jessica M. Phillips<sup>4</sup>, Aspen T. Reese<sup>5</sup>, Sudipta Majumdar<sup>1</sup>, Peter R. Girguis<sup>5</sup>, Colin  
8 L. Raston<sup>4</sup>, Gregory A. Weiss<sup>1,2,3 \*</sup>

9  
10 <sup>1</sup> Department of Chemistry, University of California, Irvine, California, United States of America  
11  
12 <sup>2</sup> Department of Molecular Biology and Biochemistry, University of California, Irvine, California, United  
13 States of America  
14  
15 <sup>3</sup> Department of Pharmaceutical Sciences, University of California, Irvine, California, United States of  
16 America

17  
18 <sup>4</sup> Flinders Institute for Nanoscale Science and Technology, College of Science and Engineering, Flinders  
19 University, Adelaide, South Australia, Australia  
20

21 <sup>5</sup> Department of Organismic and Evolutionary Biology, Harvard University, Cambridge, Massachusetts,  
22 United States of America  
23

24 <sup>#a</sup>Department of Chemical Engineering and Biotechnology, University of Cambridge, Cambridge,  
25 England, United Kingdom  
26

27 \* Corresponding Author:  
28 E-mail: gweiss@uci.edu (GAW)

## 29 **Abstract**

30 DNA from formalin-preserved tissue could unlock a vast repository of genetic information stored in  
31 museums worldwide. However, formaldehyde crosslinks proteins and DNA, and prevents ready  
32 amplification and DNA sequencing. Formaldehyde acylation also fragments the DNA. Treatment with  
33 proteinase K proteolyzes crosslinked proteins to rescue the DNA, though the process is quite slow. To  
34 reduce processing time and improve rescue efficiency, we applied the mechanical energy of a vortex  
35 fluidic device (VFD) to drive the catalytic activity of proteinase K and recover DNA from American lobster  
36 tissue (*Homarus americanus*) fixed in 3.7% formalin for >1-year. A scan of VFD rotational speeds  
37 identified the optimal rotational speed for recovery of PCR-amplifiable DNA and while 500+ base pairs  
38 were sequenced, shorter read lengths were more consistently obtained. This VFD-based method also  
39 effectively recovered DNA from formalin-preserved samples. The results provide a roadmap for exploring  
40 DNA from millions of historical and even extinct species.

## 41 **Introduction**

42 Archived biological samples offer an important source of genetic information for diverse fields including  
43 evolutionary biology, ecology, phylogenetics, biodiversity, and epidemiology [1-2]. Samples, from  
44 hydrated tissues to whole organisms, have historically been preserved in aqueous formaldehyde (3.7 to  
45 4% solution of formaldehyde in water, termed formalin). In many cases, these specimens are the only  
46 remaining samples that could provide genetic information about the organisms, including their  
47 microbiomes, environments, diets, and other attributes – all from the moment of sample preservation [3-  
48 5]. This preservative, however, hinders DNA amplification and sequencing with the sample [6]. Thus, new  
49 methods to recover DNA from formalin-fixed specimens could advance our ability to access the genetic  
50 information in these samples, and advance our understanding of how organisms and ecosystems have  
51 responded to natural and anthropogenic changes over time. For example, formalin-fixed specimens in  
52 natural history museums could be used to elucidate the impact of environmental changes on the DNA of  
53 biological populations [1-2, 7]. DNA sequencing of such samples could address longitudinal, biological  
54 questions that may be impractical to address without the genetic information for the preserved specimens  
55 [2, 8-9].

56 For >150 years, formalin fixation has been used to effectively preserve hydrated specimens [7]. A  
57 vast repository of formalin-fixed samples exists, including at least 400 million samples at 13 large  
58 institutions [1]. Marine organisms are particularly well-preserved in this aqueous preservative, as it retains  
59 morphological features well, enabling more detailed taxonomic studies. Aqueous formaldehyde is also  
60 advantageous in that it stops parasitic microbial growth [10]. However, preserving samples in formalin  
61 fixation damages DNA [11-12]. Covalent modification of DNA bases by the electrophilic formaldehyde  
62 drives base deglycosylation, and the resultant abasic sites in DNA can cause strand breakage [13].  
63 Additionally, long duration storage often incurs DNA fragmentation, independent of formalin [14].  
64 Fragments from both mechanisms increase the amount of DNA template required for PCR amplification  
65 of longer targets, and can also inhibit PCR [15-16].

66 Intrastrand and protein-DNA crosslinks introduced by formaldehyde can also block PCR and DNA  
67 sequencing [17-18]. Protein-DNA crosslinks result from nucleophilic attack on formaldehyde by proteins'  
68 primary amines to yield imines and iminium ions. These groups can then react with the less nucleophilic  
69 primary amines of DNA bases, particularly from guanine, resulting in a protein-DNA crosslink (Fig 1) [19-  
70 20]. Due to the high density of amines found on the surface of proteins and DNA, each DNA-protein  
71 complex can become crosslinked multiple times. Additionally, formalin-fixed cells cannot repair the slow  
72 process of cytosine deamination to uracil [11, 21]. During PCR amplification, adenine can be incorporated  
73 as the incorrect complement to degraded cytosine, resulting in point mutations [11]. In summary, DNA  
74 damage caused by preservation results in short templates for PCR and low-quality, error-prone DNA  
75 sequences.

76  
77 **Fig 1. Schematic of formalin-induced crosslink formation and the removal of crosslinked proteins**  
78 **by treatment with proteinase K. (A)** A protein amine can nucleophilically attack the formaldehyde  
79 carbonyl to yield an iminium ion, which can then react with another primary amine from DNA, RNA, or  
80 proteins to form a crosslink. This crosslink reaction is in reversible dynamic equilibrium [10, 21]. **(B)**  
81 Treatment with a protease, proteinase K, allows free DNA (fDNA) recovery. Here, Nuc designates an  
82 amine nucleophile from the DNA.

83       Despite the immense challenges that are associated with formalin fixation, much effort has been  
84       dedicated to developing techniques for sequencing these irreplaceable samples (DNA recovery methods  
85       from formalin-fixed tissue are summarized in Table 1). Most current methods for recovering DNA from  
86       formalin-fixed organisms use proteinase K, a thermostable serine protease with broad substrate  
87       specificity [22], to digest crosslinked proteins and eliminate most crosslink-associated blockages [21-23].  
88       However, even at the enzyme's optimum temperature ( $49 \pm 2$  °C), the free DNA (fDNA) recovery rate  
89       from this method is low at approximately 4.4% per hour; additionally, the enzyme's half-life is limiting at  
90       approximately 11.3 h [21-22]. At room temperature ( $\approx 22$  °C), the proteolytic reaction rate yields only 1.1%  
91       fDNA per hour [24]. DNA can also be recovered from formalin-fixed tissue with a 0.1 M NaOH (pH 12)  
92       buffer treatment at 120 °C for 25 min [7, 25]. However, these harsh conditions can further damage the  
93       DNA through Brønsted base-caused strand cleavage; therefore, this approach is most valuable in cases  
94       where there is an excess of tissue to be digested, and is highly inappropriate for most delicate, longer-  
95       preserved samples. Notably, the current reactions to liberate DNA are harsh, low-throughput, low  
96       yielding, and time consuming. Mild methods to increase DNA recovery and purification for PCR  
97       amplification and subsequent DNA sequencing could revolutionize the study of a wide range of museum  
98       specimens.

99       **Table 1.** Current methods for formaldehyde crosslink removal & DNA recovery from formalin-fixed  
100      specimens.

Method	Temperature (°C)	Time (h)
proteinase K treatment <sup>[26]</sup>	56	~17
proteinase K treatment in Tris-NaCl- EDTA-SDS buffer <sup>[27]</sup>	55	68
hot alkali buffer treatment <sup>[7][25]</sup>	100 to 120	0.4 to 0.7
Cetyltrimethylammonium bromide (CTAB) & proteinase K <sup>[28]</sup>	65 & 56	0.5 & 1-72
QIAamp DNA Mini Kit <sup>[28]</sup>	56	not reported
QIAamp DNA FFPE Kit <sup>[28]</sup>	56 & 90	not reported

101       We posit that judicious application of mechanical energy could address this challenge.  
102       Specifically a vortex fluidic device (VFD) directs controlled mechanical energy into solution to accelerate  
103       enzyme-catalyzed reactions [29]. This thin film microfluidic platforms can disrupt membranes and drive  
104       protein folding [30], and potentially assist with the deaggregation, and solubilization of formalin-fixed  
105       samples in addition to acceleration of enzyme activity. Here, we tested the efficacy of using a VFD to

107 accelerate proteinase K activity, and increase the process throughput and efficiency of extracting DNA  
108 from formalin-fixed specimens (Fig 2). Thus, we optimized the recovery of fDNA from formalin-fixed  
109 specimens through VFD and post-processing purification. Our results suggest that this method recovers  
110 fDNA with 40 to 85% greater yields than conventional methods without requiring harsh conditions, and  
111 can decrease treatment time from days to hours.

## 112 **Protocol**

## 113 **Reagents**

114 • Proteinase K (Promega, cat. no. V3021, lyophilized)

115 • Sodium dodecyl sulphate (SDS) (Fisher Bioreagents, cat no. BP8200-5)

116 • Tris hydrochloride (Fisher Bioreagents, cat. no. BP153-1)

117 • Calcium chloride (Fisher Chemical, cat no. C614-500)

118 • Glycerol (ACS reagent, cat. no. G7893-4L)

119 • Ethylenediaminetetraacetic acid (EDTA) (Acros Organics, cat. no. 147850010)

120 • Nitrogen (Liquid) (Airgas Healthcare, cat no. UNI977)

121 • Ethanol (200 proof, Molecular Biology Grade) (Fisher Scientific, cat. no. BP2828-500)

122 • Clean & Concentrator Kit (Zymo Research, cat. no. D4006)

## 123 **Equipment**

124 • Vortex Fluidic Device v.2 (VFD) (Vortex Fluidic Technologies)

125 • Microliter pipettes (1000 µL, 200 µL, 20 µL, and 10 µL)

126 • Refrigerated, tabletop centrifuge

127 • Vortex mixer

128 • Mortar & pestle

129 • Hemostat

130 • Forceps

131 • Razorblades

132 • Eppendorf tubes (1.7 mL)

## 133 Reagent setup

134 **Critical Step:** Nanopure water (ddH<sub>2</sub>O) is used for all buffers and solutions. Buffers are autoclaved or  
135 sterile-filtered, if containing SDS, prior to addition of enzymes and use. Enzyme-containing solutions are  
136 stored at -80 °C.

137

138     • **Proteolysis buffer** 20 mM Tris-HCl, 50 mM EDTA, 1% w/v SDS, pH 8.0<sup>[31]</sup>

139     • **Proteinase K solution** 10 mg/mL proteinase K, 20 mM Tris-HCl, 1 mM CaCl<sub>2</sub>, 50% glycerol, pH  
140           8.0

141

## 142 Procedure

### 143 Tissue sample preparation. Timing: ≈1 h

144 1. After removal of a small portion (≈5 to 10 g) of the preserved biological tissue from the preservative,  
145 immerse the tissue in liquid nitrogen until frozen, and grind with a mortar and pestle for ≈1 min. The  
146 small pieces of ground tissue are aliquoted (≈1 to 1.5 g) into Eppendorf tubes (henceforth termed  
147 tubes).

148 **Safety Note:** Exercise caution when utilizing a sharp edge to prevent puncturing or cutting personal  
149 protective equipment or skin.

150 **Pause Point:** At this stage, the sample can be stored at -80 °C for later processing.

151 2. On an autoclaved glass surface, mince the formalin-fixed tissue sample with a flame-sterilized  
152 razorblade held by a sterilized hemostat for ≈5 min.

153 **Safety Note:** Exercise caution when utilizing a sharp edge to prevent puncturing or cutting personal  
154 protective equipment or skin.

155 **Critical Step:** This step increases the surface area to volume ratio of the tissue and, thus, improves  
156 the proteinase K access to the sample.

157 3. To remove the preservative fluid, wash the sample three times with the proteolysis buffer (1 mL). For  
158 each wash step, briefly vortex, centrifuge (15 krcf, 3 min), and decant the samples. If required, an  
159 addition centrifugation (15 krcf, 1 min) can remove any residual buffer.

160 **VFD treatment. Timing: ≈1 h**

161 4. Transfer the ground, minced tissue to the bottom of an autoclaved 20 mm VFD sample tube. Add  
162 proteolysis buffer (950 µL) and then proteinase K solution (50 µL).

163 5. Seal the VFD sample tube with a rubber septum, and use the VFD to spin the sample (7 krpm, 1 h,  
164 RT).

165 **Critical Step:** This rotational speed is optimal for fDNA amplification and sequencing.

166 **Sample post-processing and purification. Timing: ≈1.5 h**

167 6. Following VFD processing, immediately transfer the sample, including both the processed tissue and  
168 solution, from the VFD sample tube to a new tube.

169 7. Immediately, centrifuge the sample (15 krcf, 5 min, RT) to remove the tissue. Transfer the  
170 supernatant to a clean tube.

171 8. Incubate the supernatant on wet ice for 30 minutes.

172 **Critical Step:** A white precipitate (SDS) collects at the bottom of the tube. The presence of SDS  
173 negatively affects PCR yields and subsequent purification of fDNA.

174 9. Immediately, centrifuge the sample (15 krcf, 10 min, 4 °C) to remove SDS, and transfer the  
175 supernatant to a new tube without disturbing the SDS pellet.

176 **Critical Step:** The supernatant must be transferred immediately following centrifugation to prevent  
177 resolubilization of SDS.

178 **Pause Point:** At this stage, the sample may be frozen at -20 or -80 °C for later analysis.

179 10. Process 400 µL of the supernatant with a Zymo DNA Clean & Concentrator Kit, according to the  
180 manufacturer's instructions.

181 **fDNA quantification and characterization. Timing: ≈8 h**

182 11. The isolated fDNA can be used for further amplification, characterization, quantification, and  
183 sequencing.

## 184 Materials & methods

185 One adult male Lobster (*H. americanus*) was purchased in February 2017 from a local lobster fishery in  
186 Boston, MA. The lobster was euthanized by quickly severing the ganglia behind the eyes with a sharp  
187 knife. The body was then placed whole in a solution of 3.7% formaldehyde in 0.9 M phosphate-buffered  
188 saline (which approximates the salinity of seawater). The lobster was maintained at room temperature for  
189 one month, and then shipped to the University of California Irvine in March 2017. All lobster trails shown  
190 here have used muscle recovered from the chelipeds (primary claws), which have remained in formalin  
191 for the two-year duration of this study. For experimental treatments, the lobster claw tissue was  
192 processed according to the procedure described above.

193 Proteinase K (Promega, V3021, lyophilized) was solubilized and diluted to 10 mg/mL in storage  
194 buffer (20 mM Tris-HCl, 1 mM CaCl<sub>2</sub>, 50% glycerol, pH 8.0).

195 For DNA isolation, 100 ( $\pm 1$ ) mg of lobster tissue samples were utilized. Tissue preparation, VFD  
196 processing, and DNA purification used methods described above. In the experiments reported here, the  
197 VFD was operated in the confined, not continuous flow, mode [32-33]; specifically, 1 mL volumes were  
198 used. The negative control samples consisted of identical tissue samples and treatment but were not  
199 subjected to VFD processing. A positive control contained VFD-processed fresh lobster tissue.  
200 Additionally, fixed and fresh lobster tissue were processed overnight at 56 °C without the VFD for the  
201 conventional method controls, based on Table 1. Finally, intermediate controls combined the conventional  
202 and VFD-mediated methods to minimize the number of variables changed per experiment. These  
203 intermediate controls consisted of fixed and fresh lobster processed overnight (as in the conventional  
204 method) at room temperature (as in the VFD-mediated method) without use of the VFD.

205 The positive controls for PCR quantification were DNA obtained from fresh (non-formalin-fixed),  
206 ground lobster claw tissue. The DNA recovery from this sample applied Chelex 100 Resin (Bio-Rad, 10%  
207 w/v in 500  $\mu$ L in ddH<sub>2</sub>O) with the manufacturer's protocol. The mixture of a tissue fragment and resin was  
208 vortexed and centrifuged briefly before incubation at 90 to 95 °C for 20 to 35 min. Following another brief  
209 vortexing and centrifugation, the supernatant was isolated as the positive control for lobster fDNA.

210 DNA extraction yields were compared by quantitative PCR (qPCR) (Bio-Rad iCycler). For PCR,  
211 reaction mixtures (10  $\mu$ L) applied the Phusion DNA polymerase (0.2 U final concentration, New England  
212 Biolabs) and buffer (5 $\times$  diluted final concentration, New England Biolabs), DMSO (10% v/v final  
213 concentration), dNTPs (0.5 mM each final concentration, New England Biolabs), primers (8-33 ng each  
214 final concentration, Integrated DNA Technologies) (Table 2), and SYBR Green I dye (10,000 $\times$  diluted final  
215 concentration, Thermo Fisher Scientific). A PCR was performed with 1 cycle of 94 °C for 5 min followed  
216 by 40 to 50 cycles of 94 °C for 1 min, 60 °C for 1 min, and 72 °C for 2 min, followed by 1 cycle of 72 °C for  
217 5 min.

218 **Table 2.** PCR primer sequences and annealing temperatures.

Gene Target: mitochondrial ATP synthase		Primer	Annealing Temperature (est.) (°C)
579 bp	Forward	GGGTTACTTTTATTCCCTACCTTATTGAGC	60
	Reverse	GGCATATAAAGTCCTAGAACAGCAAATACATACG	
183 bp	Forward	GGGTTACTTTTATTCCCTACCTTATTGAGC	60
	Reverse	CAGCCCGAGAGTGTATTGAATATAATAAAC	

219  
220 The recovered fDNA from the formalin-fixed lobster was quantified by UV-Vis absorbance. The  
221 absorbance spectra of the samples, diluted in ddH<sub>2</sub>O (1:50), were measured (Jasco V-730  
222 Spectrophotometer). The spectra were recorded from 200 to 400 nm, in triplicate (technical replicates),  
223 with a scanning speed of 200 nm/min and intervals of 0.5 nm with ddH<sub>2</sub>O as the blank. Two buffer only  
224 controls examined the reaction mixture without lobster tissue. The first was processed in the VFD (7.5  
225 krpm, 1 h, RT), and the second did not use VFD processing. The 1 kb Plus DNA Ladder (10  $\mu$ g, 1000  $\mu$ L)  
226 (Thermo Fisher Scientific, 1.0  $\mu$ g/ $\mu$ L) was used to estimate DNA sizes and concentrations; a positive  
227 control applied DNA from fresh lobster tissue extracted with Chelex 100 Resin, as described above.

228 A SYBR Green I fluorescence assay also quantified the dsDNA concentration [34]. To derive a  
229 DNA concentration calibration curve, a 1 kb Plus DNA Ladder (Thermo Fisher Scientific, 1.0  $\mu$ g/ $\mu$ L) was  
230 diluted to concentrations of 0 ng/ $\mu$ L to 1.25 ng/ $\mu$ L. These dilutions (100  $\mu$ L) and SYBR Green I dye (100  
231  $\mu$ L, Thermo Fisher Scientific, 1250 $\times$  diluted in ddH<sub>2</sub>O) were added to a black, clear-bottom 96-well plate  
232 (Corning, 3615). The fluorescence of each well was measured ( $\lambda_{ex}$  485 nm,  $\lambda_{em}$  550 nm, Bandwidth 20  
233 nm, Gain 50). The fluorescence of fDNA from the fixed lobster samples (100 $\times$  diluted) were similarly  
234 measured, and the dsDNA concentrations were estimated using the calibration curve shown in S4 Fig.

## 235 Results and discussion

236 Conventional methods applying proteinase K to remove protein-DNA crosslinks require >17 h [26-27],  
237 and typically the reaction runs for >1 day. Here we report enzyme acceleration techniques via VFD  
238 mechanical stimulation to enable DNA recovery in <2 h from lobster claw tissue (*H. americanus*)  
239 preserved in formalin (3.7% formaldehyde in phosphate-buffered saline, a condition iso-osmotic with  
240 seawater). Key variables requiring optimization included mechanical breakage of the tissue sample,  
241 length of fDNA sequences to be amplified, and rotational speed of the VFD. As observed for other VFD-  
242 enhanced enzymes [29], proteinase K activity can be accelerated using a VFD. The approach allows  
243 recovery of free DNA (fDNA) from formalin-fixed samples. The rotational speed of the tube in the VFD  
244 determines the level of shear, micro-mixing, and fluid dynamics experienced by the thin film of liquid [32].  
245 The tilt angle of the VFD can be important, and 45° relative to the horizontal is the optimal tilt angle for a  
246 myriad of applications, including accelerating enzymatic reactions [29, 32].

247

248 **Fig 2. Schematic of the VFD-mediated fDNA recovery technique.** (A) The protocol begins with Vortex  
249 Fluidic Device (VFD) treatment (7 krpm, room temperature, abbreviated RT, 1 h) of a mixture of  
250 proteinase K and the frozen, then broken-up tissue. The reaction mixture is next processed to remove  
251 solids and DNA polymerase inhibitors. The recovered fDNA is then purified and concentrated. Finally, the  
252 DNA is amplified, quantified, and characterized by (B) qPCR and (C) DNA sequencing of the samples.  
253 Larger versions of panels B and C are provided in S1 and S2 Figs. Threshold cycle ( $C_t$ ) and endpoint  
254 fluorescence values are given in S1 Table.

255 Mechanical breakage of the tissue sample emerged as a key variable for efficient and robust  
256 isolation of fDNA. Smaller fragments increase the surface area to volume ratio, allowing greater efficiency  
257 of proteinase K digestion. Also, the VFD removes solids from solution by centrifugation, and, therefore,  
258 breaking the tissue sample into small fragments improves the efficiency of VFD-mediated fDNA recovery.  
259 The formalin-fixed tissue was first frozen in liquid nitrogen then ground into small particles using a clean  
260 mortar and pestle. When extracted using traditional extraction approaches, the ground material yielded  
261 modest and inconsistent quantities of fDNA (Fig 2 and S1 Table). The lack of reproducibility suggested a

262 need for further mechanical breakdown of the tissue. Beadbeating and sonication increased the observed  
263 breakdown of tissue, but both methods failed to improve PCR product yields (data not shown). These  
264 failures may be due to the fact that sonication or the resultant heat generation through cavitation could  
265 introduce additional breaks in the DNA. However, we found that a second, mincing step with a sterile,  
266 new razorblade consistently improved fDNA recovery (Fig 4).

267 Also, the length of the amplified DNA proved critical for consistent recovery from formalin-fixed  
268 samples. In initial experiments, we amplified a 579 bp sequence of fDNA. The amplified DNA was the  
269 correct lobster sequence (Fig 2, Fig 4, and S2 Fig), but this long fragment proved difficult to amplify  
270 repeatedly. Thus, primers targeting a 183 bp sequence were used for all further experiments reported  
271 here. The shorter target amplicon decreased the chance of DNA fragmentation damaging the sequence  
272 and preventing PCR amplification. As expected, DNA sequencing quality in the non-VFD control reactions  
273 was difficult to monitor; only three out of thirteen cumulative control amplification reactions yielded fDNA  
274 detectable by gel electrophoresis.

275 The final parameter optimized for fDNA extraction was the rotational speed of the VFD. Previous  
276 studies with the VFD have demonstrated that acceleration of enzymatic catalysis occurs at rotational  
277 speeds between 5 and 9 krpm with the VFD at a 45° tilt angle [29]. Hypotheses attribute the enzymatic  
278 acceleration phenomena to two interconnected actions. First, the periodic change in the thickness of the  
279 thin fluid film present in the VFD, results in intense micro-mixing and high mass transfer. Second, the  
280 Faraday waves arising from this periodic change contribute to zones of high and low pressure within the  
281 reaction mixture and, accordingly, the enzyme present in solution. The pressure oscillations could  
282 increase substrate accessibility and removal of product from the enzyme active site, which also benefit  
283 from the high mass transfer of the VFD.

284 To identify optimal speeds for fDNA recovery, a systematic assessment of rotational speeds  
285 between 5 and 9 krpm at intervals of 1 krpm was conducted. Heterogeneity inherent to pulverized tissue  
286 imparts idiosyncratic and uncontrollable variables into this optimization and subsequent isolation of fDNA.  
287 Thus, the yields of fDNA, as determined by UV-Vis spectrophotometry, were sometimes inconsistent (It is  
288 well known that absorption of 260 nm is a proxy for DNA concentrations in solution, whereas the ratio of  
289 absorbances at 260:280 nm serves as an indicator of DNA purity). Though absorbance at 260 nm

290 increased for the VFD-processed samples at various rotational speeds relative to the non-VFD-processed  
291 negative control, the ratio of 260:280 nm absorbances was significantly <1.8 for all rotational speeds (Fig  
292 3 and S3 Fig), which likely indicates inclusion of protein in the VFD-treated samples [35]. The DNA-  
293 associated, absorbance at 260 nm was greatest for the samples processed at 8 krpm. This rotational  
294 speed is within the VFD-based rate enhancement zone for reactions in aqueous solvents. That said, the  
295 highest, most consistently observed PCR yields were obtained for the rotational speed of the VFD of 7  
296 krpm (which is discussed in more detail below; see Fig 2, Fig 4, S1 Fig, S2 Table, and S5 Fig).

297

298 **Fig 3. Quantification for optimizing the VFD rotational speed for fDNA yields.** After proteinase K  
299 and VFD treatment at the indicated speeds, **(A)** absorbance at 260 nm and **(B)** the ratio of absorbances  
300 260:280 nm quantifies DNA and protein yields, respectively, with positive and negative controls. Full UV-  
301 vis spectra for these samples are shown in S3 Fig. SYBR Green I fluorescence-quantified **(C)** dsDNA  
302 concentration and **(D)** fold increase in dsDNA yield between non-VFD-processed and VFD-processed  
303 samples. The negative control indicates samples not subjected to VFD processing. Buffer only controls  
304 lacked lobster tissue. The positive controls included DNA that had not been formalin fixed. Additional  
305 controls demonstrated a conventional method and an intermediate method (processing time of the  
306 conventional method and temperature of the VFD-mediated method) used to process fixed and fresh  
307 tissue without the VFD. The error bars designate the standard deviation for sample measurements at the  
308 indicated condition (technical replicates,  $n = 3$ ).

309 To more robustly quantify the concentration of double-stranded DNA (dsDNA) in the fDNA, a  
310 fluorescence-based DNA intercalating assay was performed using SYBR Green I dye. Samples were  
311 diluted to reach the dye's linear range, and the sample fluorescence ( $\lambda_{\text{ex}} 485 \text{ nm}$ ,  $\lambda_{\text{em}} 550 \text{ nm}$ ) was  
312 measured against a standard curve to determine the concentrations of the rescued dsDNA. The assay  
313 demonstrated that VFD-processed samples yielded 40 to 85% more dsDNA than the control, non-VFD  
314 processed sample (Fig 3). Thus, the VFD improved the rescue of dsDNA from formalin-fixed tissue  
315 compared to the non-VFD-treated negative control.

316 Moreover, and most importantly, DNA recovered via VFD-enhanced extraction were amenable to  
317 amplification via PCR and quantitative PCR (or qPCR). Post-VFD treatment, samples were purified and

318 concentrated with a Zymo™ DNA Clean & Concentrator Kit, which removes DNA polymerase inhibitors  
319 and proteins [16, 36]. Using the fDNA samples and qPCR, we observed reproducible amplification of an  
320 183 bp target amplicon from the gene encoding ATP synthase from samples processed with a VFD  
321 rotating at either 6 or 7 krpm (Fig 4, Table 2). Paradoxically, these speeds had lower fDNA yields when  
322 compared to the 8 krpm (as described above; see Fig 3a-b). However, the 8 krpm treated DNA would  
323 amplify <50% of the time (n = 8, shown in S5 Fig). Though yields were greater, the more aggressive  
324 treatment is apparently liberating other compounds that can be problematic to PCR amplification (this  
325 phenomena has also been seen in algal cells and more) [37]. Additionally, it is plausible that greater VFD  
326 rotational speeds could result in both greater yields and further fragmentation of fDNA, which could  
327 explain the higher DNA concentrations, but lower amplification efficacy [16].

328 From the formalin-fixed samples, the 7 krpm VFD-processed DNA sample yielded the highest  
329 levels of fDNA amplification as measured by qPCR. For example, on average  $94\pm4\%$  of the endpoint  
330 positive control fluorescence signal was obtained with a low threshold cycle ( $C_t$ ) value, averaging  
331  $35.4\pm0.7$  cycles (S2 Table). Comparatively, the no template controls (NTC) did not surpass the threshold  
332 in two of three trials, and their fluorescence averaged  $10\pm10\%$  of the endpoint positive control  
333 fluorescence signal (S2 Table). The lower  $C_t$  values demonstrated a greater yield of DNA. Furthermore,  
334 the PCR product of the fDNA rescued from the 7 krpm VFD-processing condition could readily be  
335 sequenced via Sanger sequencing. This sequence exhibited 99.5% homology to the expected sequence  
336 [38]. The 6 krpm-processed sample offered a decreased yield of amplified DNA. Notably, PCR  
337 amplification failed for the non-VFD-treated sample.

338 The data herein illustrate the efficacy of our new VFD-enabled method for fDNA recovery. We  
339 have demonstrated the successful amplification of fDNA from biological specimens treated with  
340 formaldehyde. We have also shown that fDNA can be used to great effect with appropriately designed  
341 qPCR assays. Therefore, we are optimistic that this method presents a potentially valuable method for  
342 increasing the throughput of fDNA recovery. Increasing the rate at which fDNA can be recovered is a  
343 timely pursuit, as there are tens of millions of formalin-fixed samples stored in museums around the world.  
344 These organisms provide a “time capsule” of sorts, revealing the genomic adaptations of organisms to a  
345 pre-industrial world. Indeed, museum specimens may become our first tool for understanding the extent

346 to which anthropogenic factors are shaping our biosphere. It is also important to note that fDNA is,  
347 unfortunately, subject to irreparable damage and fragmentation, and any PCR-based amplification from  
348 such samples will always be highly dependent on rescue conditions, primer design (especially amplicon  
349 length), tissue mincing, and other factors. The VFD method here may help investigators tap into this  
350 enormous genetic repository.

351

352 **Fig 4. Amplification of an 183-bp fDNA target from the ATP synthase gene of the lobster**  
353 **mitochondrial genome. (A)** Quantitative PCR and **(B)** agarose DNA gel electrophoresis identified 7  
354 krpm as the optimal VFD rotational speed for qPCR amplification. Threshold cycle and endpoint  
355 fluorescence values are provided in S2 Table. The variable-rotational speed PCR reactions were  
356 compared to a no template control (NTC), a fresh lobster DNA positive control (+), and a non-VFD-  
357 processed negative control (-). **(C)** The 7 krpm VFD-processed qPCR product (\*) was subjected to  
358 Sanger sequencing; a mutation (G2728A, GenBank No. HQ402925) was observed (highlighted).

359 **Availability**

360 Genbank is a collection of gene and genome sequences in the National Center for Biotechnology  
361 Information database (<https://www.ncbi.nlm.nih.gov/genbank/>).

362 **Author information**

363 **ORCID**

364 CA Totoiu: 0000-0001-9839-8894

365 JM Phillips: 000-0001-5673-0879

366 AT Reese: 0000-0001-9004-9470

367 S Majumdar: 0000-0001-6738-2267

368 PR Girguis: 0000-0002-3599-8160

369 CL Raston: 0000-0003-4753-0079

370 GA Weiss: 0000-0003-0296-9846

## 371 **Acknowledgements**

372 We gratefully thank UCI's Department of Molecular Biology and Biochemistry for access to the qPCR  
373 thermocycler.

## 374 **Funding**

375 This work was supported by the National Human Genome Research Institute (NHGRI) of the National  
376 Institutes of Health [1R01HG009188-01 to G.A.W.]; the Star Family Foundation Challenge for Promising  
377 Scientific Research [to A.T.R. and P.R.G.]; and the University of California at Irvine's Undergraduate  
378 Research Opportunities Program and Summer Undergraduate Research Program [to C.A.T.]. Funding for  
379 open access charge: NHGRI.

## 380 **Conflict of interest**

381 The authors declare no competing financial interests. Debut Biotechnology, a company co-founded by  
382 Dr. Weiss, has licensed the VFD technology for different applications.

## 383 **References**

384 [1] Holmes,M.W., Hammond,T.T., Wogan,G.O., Walsh,R.E., LaBarbera,K., Wommack,E.A.,  
385 Martins,F.M., Crawford,J.C., Mack,K.L., Bloch,L.M. and Nachman,M.W. (2016) Natural history  
386 collections as windows on evolutionary processes. *Mol. Ecol.*, **25**, 864–881.

387 [2] Suarez,A.V. and Tsutsui,N.D. (2004) The value of museum collections for research and society.  
388 *BioScience*, **54**, 66–74.

389 [3] Pergams,O.R.W. and Nyberg,D. (2001) Museum collections of mammals corroborate the exceptional  
390 decline of prairie habitat in the Chicago region. *J. Mammal.*, **82(4)**, 984-992.

391 [4] Lens,L., Van Dongen,S., Norris,K., Githiru,M. and Matthysen,E. (2002) Avian persistence in  
392 fragmented rainforest. *Science*, **298(5596)**, 1236-1238.

393 [5] Carroll,S.P. and Boyd,C. (1992) Host race radiation in the soapberry bug: natural history with the  
394 history. *Evolution*, **46(4)**, 1052-1069.

395 [6] Greer,C.E., Lund,J.K. and Manos,M.M. (1991) PCR amplification from paraffin-embedded tissues:  
396 recommendations on fixatives for long-term storage and prospective studies. *PCR Methods Appl.*,  
397 **1(1)**, 46-50.

398 [7] Hykin,S.M., Bi,K. and McGuire,J.A. (2015) Fixing formalin: a method to recover genomic-scale DNA  
399 sequence data from formalin-fixed museum specimens using high-throughput sequencing. *PLoS  
400 ONE*, **10(10)**, e0141579.

401 [8] Mikheyev,A.S., Tin,M.M.Y., Arora,J. and Seeley,T.D. (2015) Museum samples reveal rapid evolution  
402 by wild honey bees exposed to a novel parasite. *Nat. Commun.*, **6**, 7991.

403 [9] Spurgin,L.G., Wright,D.J., van der Velde,M., Collar,N.J., Komdeur,J., Burke,T. and Richardson,D.S.  
404 (2014) Museum DNA reveals the demographic history of the endangered Seychelles warbler. *Evol.  
405 Appl.*, **7(9)**, 1134-1143.

406 [10] Fox,C.H., Johnson,F.B., Whiting,J. and Roller,P.P. (1985) Formaldehyde fixation. *J. Histochem.  
407 Cytochem.*, **33(8)**, 845-853.

408 [11] Do,H. and Dobrovic,A. (2015) Sequence artifacts in DNA from formalin-fixed tissues: causes and  
409 strategies for minimization. *Clin. Chem.*, **61(1)**, 64-71.

410 [12] Suzuki,T., Ohsumi,S. and Makino,K. (1994) Mechanistic studies on depurination and apurinic site  
411 chain breakage in oligodeoxyribonucleotides. *Nucleic Acids Res.*, **22(23)**, 4997-5003.

412 [13] Lindahl,T. and Andersson,A. (1972) Rate of chain breakage at apurinic sites in double-stranded  
413 deoxyribonucleic acid. *Biochemistry*, **11(19)**, 3618-3623.

414 [14] Ludyga,N., Grunwald,B., Azimzadeh,O., Englert,S., Hofler,H., Tapiro,S. and Aubele,M. (2012)  
415 Nucleic acids from long-term preserved FFPE tissues are suitable for downstream analyses.  
416 *Virchows Arch.*, **460**, 131-140.

417 [15] Didelot,A., Kotsopoulos,S.K., Lupo,A., Pekin,D., Li,X., Atochin,I., Srinivasan,P., Zhong,Q.,  
418 Olson,J., Link,D.R., Laurent-Piug,P., Blons,H., Hutchison,J.B. and Taly,V. (2013) Multiplex picoliter-  
419 droplet digital PCR for quantitative assessment of DNA integrity in clinical samples. *Clin. Chem.*,  
420 **59(5)**, 815-823.

421 [16] Dietrich,D., Uhl,B., Sailer,V., Holmes,E.E., Jung,M., Meller,S. and Kristiansen,G. (2013) Improved  
422 PCR performance using template DNA from formalin-fixed and paraffin-embedded tissues by  
423 overcoming PCR inhibition. *PLoS ONE*, **8(10)**, e77771.

424 [17] Dutta,S., Chowdhury,G. and Gates,K.S. (2007) Interstrand cross-links generated by abasic sites  
425 in duplex DNA. *J. Am. Chem. Soc.*, **129(7)**, 1852-1853.

426 [18] Vesnaver,G., Chang,C.N., Eisenberg,M., Grollman,A.P. and Breslauer,K.J. (1989) Influence of  
427 abasic and anucleosidic sites on the astability, conformation, and melting behavior of a DNA duplex:  
428 correlations of thermodynamic and structural data. *Proc. Natl. Acad. Sci. U.S.A.*, **86(10)**, 3614-3618.

429 [19] Kennedy-Darling,J. and Smith,L.M. (2014) Measuring the formaldehyde protein-DNA cross-link  
430 reversal rate. *Anal. Chem.*, **86(12)**, 5678-5681.

431 [20] Hoffman,E.A., Frey,B.L., Smith,L.M. and Auble,D.T. (2015) Formaldehyde crosslinking: A tool for  
432 the study of chromatin complexes. *J. Biol. Chem.*, **290(44)**, 26404-26411.

433 [21] Kavli,B., Otterlei,M., Slupphaug,G. and Krokan,H.E. (2007) Uracil in DNA-general mutagen, but  
434 normal intermediate in acquired immunity. *DNA Repair (Amst.)*, **6(4)**, 505-516.

435 [22] Yazawa,K., Sugahara,M., Yutani,K., Takehira,M. and Numata,K. (2016) Derivatization of  
436 proteinase K with heavy atoms enhances its thermal stability. *ACS Catal.*, **6(5)**, 3036-3046.

437 [23] Goelz,S.E., Hamilton,S.R. and Vogelstein,B. (1985) Purification of DNA from formaldehyde fixed  
438 and paraffin embedded human tissue. *Biochem. Biophys. Res. Commun.*, **130(1)**, 118-126.

439 [24] Butler,J.M., Johnson,J.E. and Boone,W.R. (2013) The heat is on: room temperature affects  
440 laboratory equipment—an observational study. *J. Assist. Reprod. Genet.*, **30(10)**, 1389-1393.

441 [25] Campos,P.F. and Gilbert,T.M.P. (2012) DNA extraction from formalin-fixed material. In  
442 Shapiro,B. and Hofreiter,M. (eds) *Ancient DNA. Methods in Molecular Biology (Methods and*  
443 *Protocols)*. Humana Press, Vol. 840.

444 [26] Munchel,S., Hoang,Y., Zhao,Y., Cottrell,J., Klotzle,B., Godwin,A.K., Koestler,D., Beyerlein,P.,  
445 Fan,J., Bibikova,M. and Chien,J. (2015) Targeted or whole genome sequencing of formalin fixed  
446 tissue samples: potential applications in cancer genomics. *Oncotarget.*, **6(28)**, 25943-25961.

447 [27] Hassani,A. and Khan,G. (2015) A simple procedure for the extraction of DNA from long-term  
448 formalin-preserved brain tissues for the detection of EBV by PCR. *Exp. Mol. Pathol.*, **99(3)**, 558-563.

449 [28] Paireder,S., Werner,B., Bailer,J., Werther,W., Schmid,E., Patzek,B. and Cichna-Markl,M. (2013)  
450 Comparison of protocols for DNA extraction from long-term preserved formalin fixed tissues. *Anal.*  
451 *Biochem.*, **439(2)**, 152-160.

452 [29] Britton,J., Meneghini,L.M., Raston,C.L. and Weiss,G.A. (2016) Accelerating enzymatic catalysis  
453 using vortex fluidics. *Angew. Chem. Int. Ed.*, **55(38)**, 11387-11391.

454 [30] Yuan,T.Z., Ormonde,C.F.G., Kudlacek,S.T., Kunche,S., Smith,J.N., Brown,W.A., Pugliese,K.M.,  
455 Olsen,T.J., Iftikhar,M., Raston,C.L. and Weiss,G.A. (2015) Shear stress-mediated refolding of  
456 proteins from aggregates and inclusion bodies. *ChemBioChem.*, **16**, 393-396.

457 [31] Hu,M., Jex,A.R., Campbell,B.E. and Gasser,R.B. (2007) Long PCR amplification of the entire  
458 mitochondrial genome from individual helminths for direct sequencing. *Nat. Protoc.*, **2(10)**, 2339-  
459 2344.

460 [32] Britton,J., Stubbs,K.A., Weiss,G.A. and Raston,C.L. (2017) Vortex fluidic chemical  
461 transformations, *Chem. Eur. J.*, **23**, 13270-13278.

462 [33] Luo,X., Al-Antaki,A.H.M., Harvey,D.P., Ruan,Y., He,S., Zhang,W. and Raston,C.L. (2018) Vortex  
463 fluidic mediated synthesis of macroporous bovine serum albumin-based microspheres. *ACS Appl.*  
464 *Mater. Interfaces.*, **10**, 27224-27232.

465 [34] Leggate,J., Allain,R., Isaac,L. and Blais,B.W. (2006) Microplate fluorescence assay for the  
466 quantification of double stranded DNA using SYBR Green I dye. *Biotechnol. Lett.*, **28(19)**, 1587-1594.

467 [35] Glasel,J.A. (1995) Validity of nucleic acid purities monitored by 260 nm/280nm absorbance ratios.  
468 *BioTechniques.*, **18(1)**, 62-63.

469 [36] Hu,Q., Liu,Y., Yi,S. and Huang,D. (2015) A comparison of four methods for PCR inhibitor  
470 removal. *Forensic Sci. Int. Genet.*, **16**, 94-97.

471 [37] Sitepu,E.K., Corbin,K., Luo,X., Pye,S.J., Tang,Y., Leterme,S.C., Heimann,K., Raston,C.L. and  
472 Zhang,W. (2018), *Bioresour Technol.*, **266**, 488-497.

473 [38] Kim,S., Lee,S.H., Park,M.H., Choi,H.G., Park,J.K. and Min,G.S. (2011) The complete  
474 mitochondrial genome of the American lobster, *Homarus americanus* (Crustacea, Decapoda)  
475 *Mitochondrial DNA*, **22(3)**, 47-49.

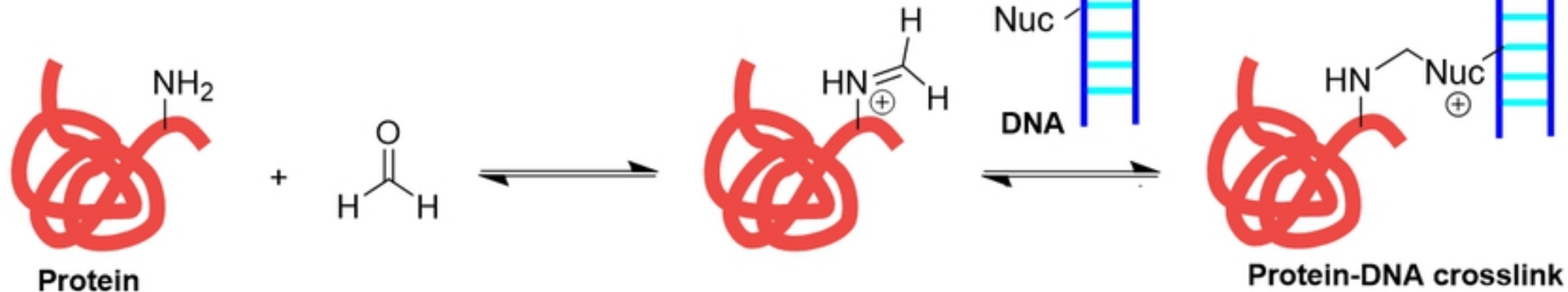
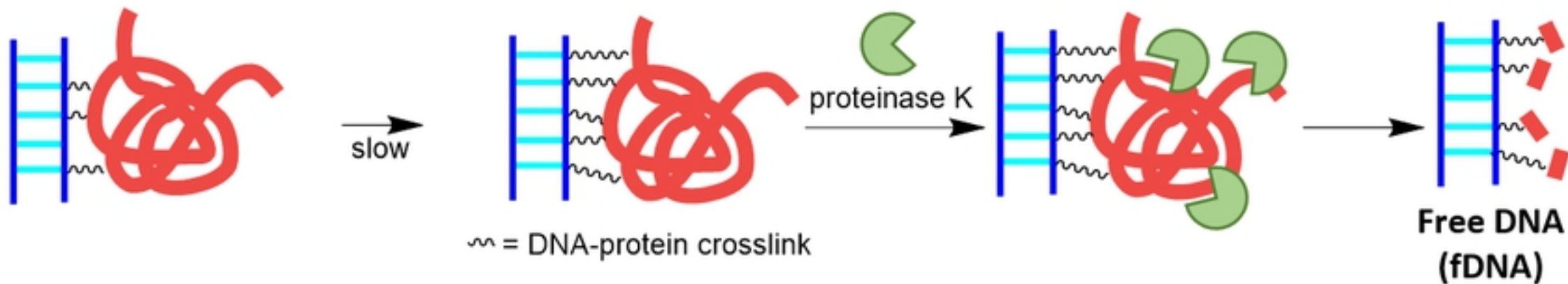
**A****B**

Figure 1

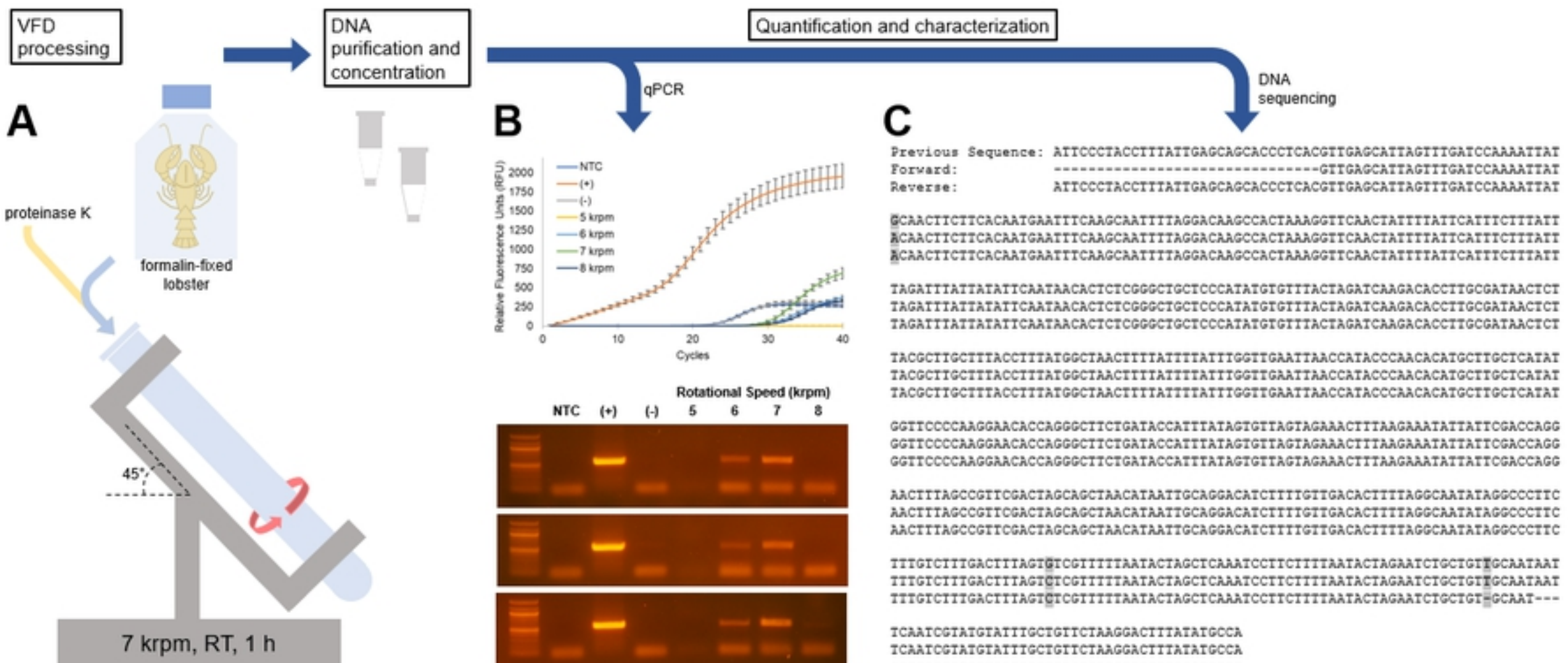


Figure 2

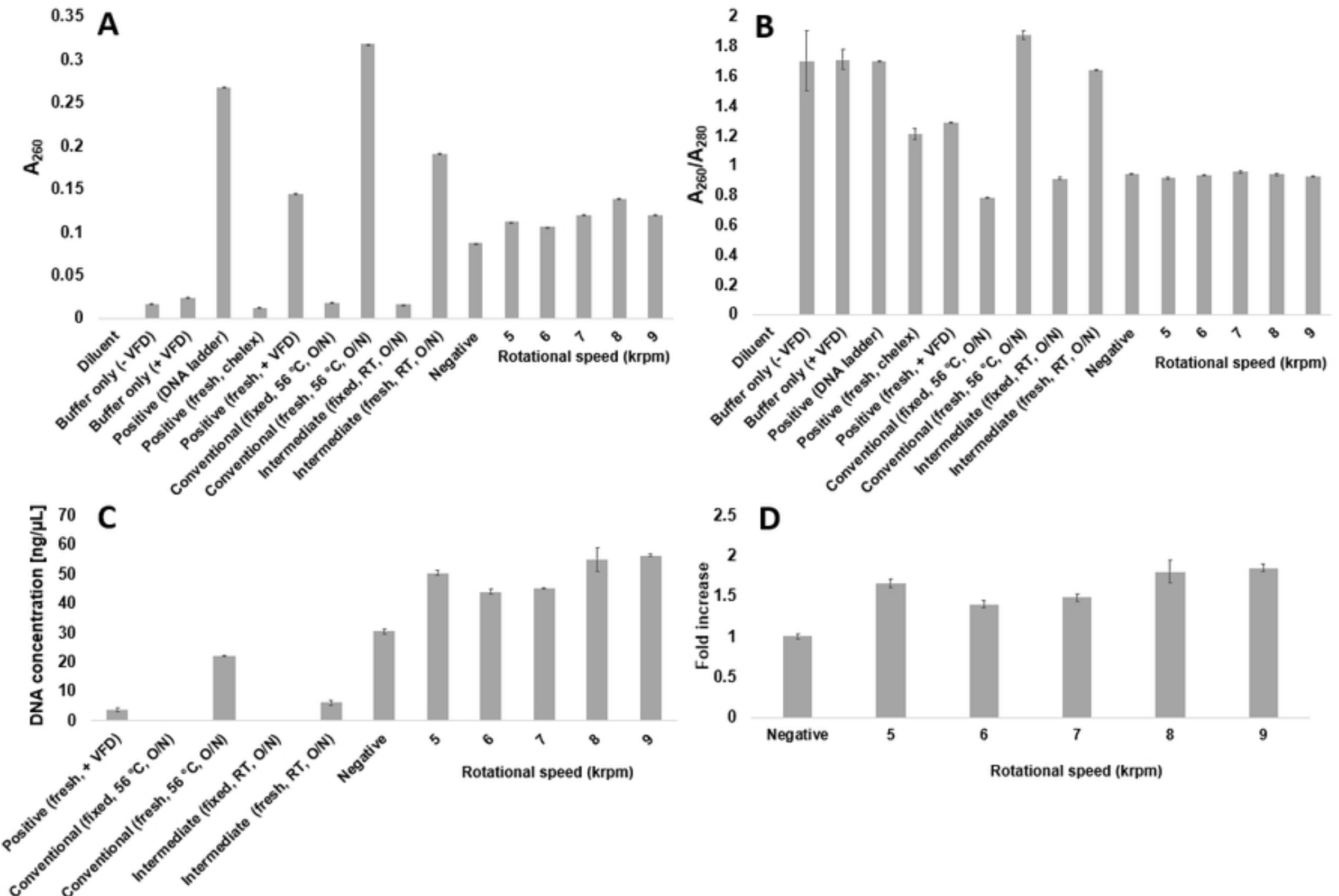
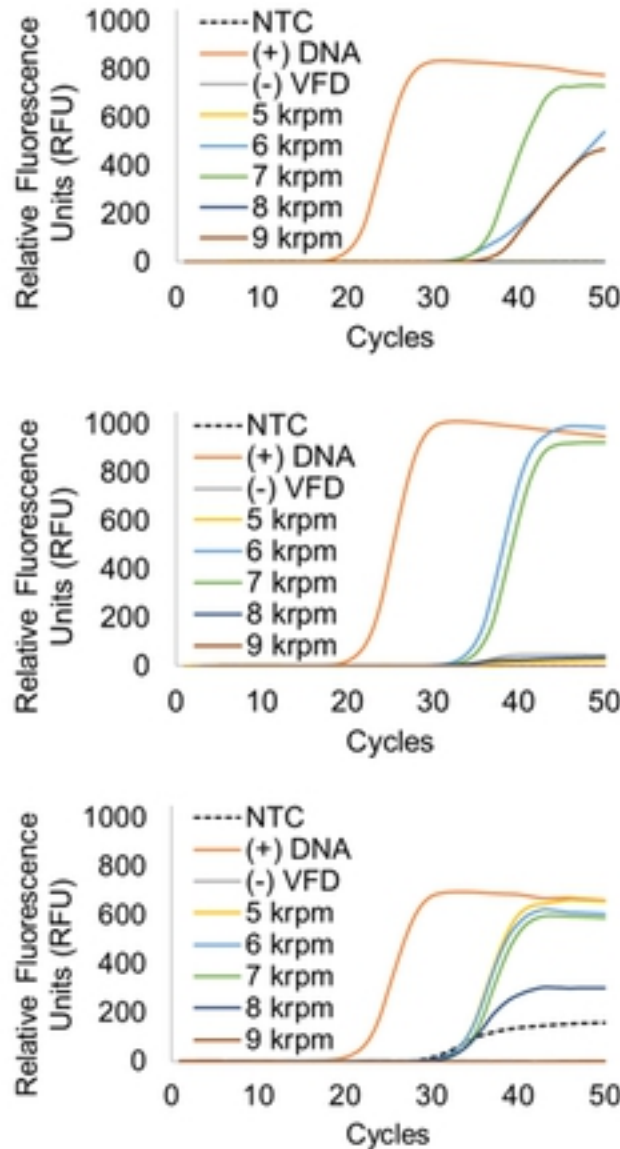
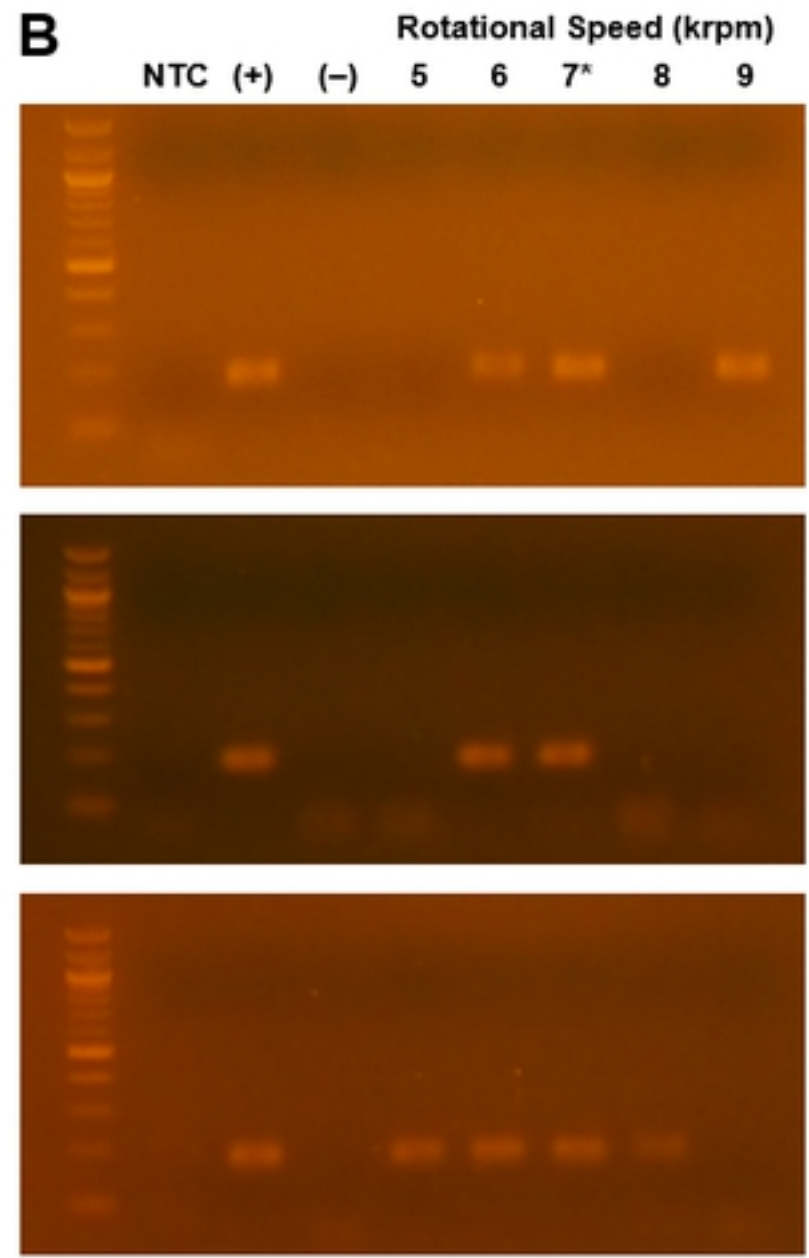


Figure 3

**A****B****C**

Previous Sequence: GGTTACTTTTATTCC  
 \*Forward: GGTTACTTTTATTCC  
 \*Reverse: -----

CTACCTTATTGAGCAGCACCTCACGTTGAGCATT  
 CTACCTTATTGAGCAGCACCTCACGTTGAGCATT  
 -----CGTTGAGCATT

AGTTTGATCCAAAATTATGCAACTTCTTCACAATGA  
 AGTTTGATCCAAAATTATACAACCTTCTTCACAATGA  
 AGTTTGATCCAAAATTATACAACCTTCTTCACAATGA

ATTTCAAGCAATTAGGACAAGCCACTAAAGGTTC  
 ATTTCAAGCAATTAGGACAAGCCACTAAAGGTTC  
 ATTTCAAGCAATTAGGACAAGCCACTAAAGGTTC

AACTATTATTATTCAATTCTTTATTAGATTATTAT  
 AACTA-----  
 AACTATTATTATTCAATTCTTTATTAGATTATTAT

ATTCAATAACACTCTCGGGCTG  
 -----  
 ATTCAATAACACTCTCGGGCTG

**Figure 4**